Applied Surface Science 476 (2019) 486–492

Contents lists available at ScienceDirect

Applied Surface Science

journal homepage: www.elsevier.com/locate/apsusc

Full Length Article

Light-emitting perovskite solar cell with segregation enhanced self doping

Dmitry Gets[a,*], Danila Saranin[b], Arthur Ishteev[a,b], Ross Haroldson[c], Eduard Danilovskiy[a], Sergey Makarov[a], Anvar Zakhidov[a,b,c]

[a] ITMO University, Department of Nanophotonics and Metamaterials, Lomonosov Str. 9, Saint-Petersburg 191002, Russia
[b] National University of Science and Technology, NUST-MISIS, Leninsky pr. 4, Moscow 119049, Russia
[c] Alan G. MacDiarmid NanoTech Institute, Department of Physics, University of Texas at Dallas, Richardson, TX 75083, USA

ARTICLE INFO

Keywords:
Mixed halide perovskite
Solar cell
LED
Dual functional
Segregation

ABSTRACT

Organic-inorganic halide perovskites recently have emerged as a promising material for highly effective light-emitting diodes (LEDs) and solar cells (SCs). Despite efficiencies of both perovskite SCs and LEDs are already among the best, the development of a perovskite dual functional device that is capable of working in these two regimes with high efficiencies is still challenging. Here we demonstrate that the dual functional device based on mixed halide perovskite $CH_3NH_3PbBr_2I$ can be switched from SC to LED with low threshold voltage $V_{th} < 2$ V by exposing to Sun at open circuit V_{oc} or at small bias voltage of $V_{pol} \sim 1$–2 V. Such photo-poling creates *in-situ* p-i-n junction via methylammonium ($CH_3NH_3^+$, MA^+) and I^-/Br^- ions migration to interfaces, lowering charge injection barriers, and self-balancing injection currents in perovskite LED. We show that before the photo-poling, the electroluminescence (EL) is highly unstable in LED regime, whereas after the photo-poling, stabilized EL exhibits unusual dynamics, increasing with time and poling cycle number, while V_{th} and injection current decrease with cycling runs. Additionally, photo-induced and current-induced halide segregation accumulates with cycling, that is found beneficial for LED, increasing its efficiency and brightness, but reversibly degrading photovoltaic performance, which can be easily recovered.

1. Introduction

The organohalide perovskite solar cells have shown superior efficiencies of > 23% and which keep growing [1], while at the same time perovskite LEDs keep demonstrating very high quantum efficiencies and bright pure colors [2]. Also, there are many works devoted to investigation of PS solar cells properties and how it can be stabilized [3–12]. This raised the question of creating the dual function device, which is a light emitting solar cell (LESC) that may show both good photovoltaic (PV) operation and good electroluminescence (EL) with high external quantum efficiency (EQE_{EL}) in the same device. However, creation of such device is challenging, because achieving both good charge collection (PV operation) and efficient charge injection (LED operation) requires complex device design or use of properly doped transport layers with specific properties.

Several approaches were already demonstrated in order to achieve such dual functionality in one monolithic single halide perovskite device [13,14] or organic based device [15]. For example, the special type of ionic electron transport layer (ETL), such as polyethyleneimine (PEI) was suggested, which has ionic conductor properties and improves charge injection by doping perovskite/ETL interface [14]. In another example, authors utilized low work function Ba cathode [13]. But these dual functional devices either had low power conversion efficiency (PCE) or irradiated EL light in IR region (while visible light EL is usually desired), or needed complex device design to achieve high performance. Summary of the previous works on light-emitting solar cells (LESCs) is shown in Table 1 with comparison to the described in present paper.

Recently, it was demonstrated by Deng [16,17] that p-i-n structure could be formed inside a perovskite layer by photo-poling. It was found that in the device under 1 Sun illumination at photogenerated open circuit voltage (V_{OC}) an internal p-i-n junction is created in the perovskite layer by movement of MA^+ and I^-/Br^- ions towards perovskite/hole transport layer (HTL) and perovskite/ETL interfaces. As a result, V_{OC} increases in 1 min timescale and improves PCE of the SC. This p-i-n structure quickly disappears by backward ionic migration, if light is switched off [16]. As we show below, similar *in-situ* p-i-n structure formation in mixed halide perovskite structures can be used not only for enhancement of PV characteristics, but also for LED operation improvement. Moreover, theoretical investigations [18]

* Corresponding author.
E-mail addresses: dmitry.gets@metalab.ifmo.ru (D. Gets), zakhidov@utdallas.edu (A. Zakhidov).

https://doi.org/10.1016/j.apsusc.2019.01.031
Received 13 September 2018; Received in revised form 29 December 2018; Accepted 3 January 2019
Available online 08 January 2019
0169-4332/

Table 1
Comparison of different approaches to Light emitting solar cells in previously reported work and in present paper.

Structure of the device	PV Parameters	EL spectrum and parameters	Mechanism of charge injection/collection	Ref.
ITO/PEDOT:PSS/ $MAPbBr_2I$ /PCBM/LiF/ Al	V_{OC} dynamically improves from 0.6 to 1 V upon light exposure due to p-i-n formation PCE = 5–8% V_{OC} = 1.08 V J_{SC} = 8 mA/cm^2 FF = 56%	LED Color changes during operation λ: 690 → 750 nm EQE_{EL} ≈ 0.03% and amplitude grows with exposure to light due to segregation of I-rich clusters. Opt. power ~ 130 μW/cm^2 and grows in time	Internal p-i-n formation in perovskite layer is induced by photo-poling at V_{OC} and higher V_{bias} with light soaking cycling for electrical field and light enhanced ionic migration in mixed halide	This work
ITO/PEDOT:PSS/ $MAPbBr_3$/PEIBIm$_4$/Ag	PCE = 1.02% V_{OC} = 1.05 V J_{SC} = 3.12 mA/cm^2 FF = 31%	λ ≈ 520–560 nm L ≈ 8000 cd/m^2 EQE_{EL} = 0.12%	Lowering barrier at ETL induced by the n-doping or by dipoles at the interface induced by PEIBIm$_4$	Kim, et al. Ref. [6]
FTO/TiO_2/m-TiO_2/ $MAPbI_3$/Spiro-OMETAD/Au	PCE = 20.8% V_{OC} = 1.16 V J_{SC} = 24.6 mA/cm^2 FF = 73%	λ = 775 nm EQE_{EL} = 0.5%	Initial p-i-n structure created by pre-doped p-HTL and n-ETL	Dongqin Bi et. al. Ref. [3]
ITO/PEDOT:PSS/pTPD/ $MAPbI_3$/PCBM/Ba/Ag	PCE = 12.8% V_{OC} = 1.08 V J_{SC} = 18.5 mA/cm^2 FF = 64%	λ = 765 nm EQE_{EL} = 0.04% Opt. power = 100 μW/cm^2	Low work function Ba cathode for increased electron injection in LED	L. Gil-Escrig et. al. Ref. [5]
FTO/TiO_2/$CsPbI_3$/Spiro-OMETAD /MoO_x/Al	PCE = 10.77% V_{OC} = 1.23 V J_{SC} = 13.4 mA/cm^2 FF = 65%	λ ≈ 700 nm	Quantum dot photoactive and emissive layer, which facilitate charge injection in LED mode	Abhishek et. al. Ref. [4]

demonstrated the importance of the optimization of transport layer parameters, particularly by adjusting the doping level and Fermi level position to the energy levels in perovskite and collecting electrodes. Manipulation of these parameters [19,20], further investigation of ionic transport in perovskite [21] and defects formation related to different perovskite point defects [22,23] are the ways for further performance increase of perovskite based devices.

Here we study a novel strategy for cheap and effective dual functional LESC based on mixed halide perovskite solar cells by demonstrating that photo-poling induced p-i-n junction can be used for switching from conventional SC mode ($V < V_{oc}$) to LED operation ($V_{bias} > V_{th}$) in a classical planar PV-structure with a simple organic ETL. Usually, PCBM or C_{60} are used as ETL in SC, but they aren't suitable for the EL operation, owing to high barrier for electron injection to a conduction band of perovskite from the low-lying lowest unoccupied molecular orbital of fullerides. In this study, to avoid this problem, we use mixed halide perovskite ($MAPbBr_2I$), since it has large enough band gap for EL in visible range, and at the same time it demonstrates enhanced ions migration. Although the mixed halide perovskite exhibits the halide segregation effect under light soaking [24–27] or biasing [28], which usually degrades characteristics of perovskite, we show here benefits of the segregation for LED operation. Indeed, such mixed halide LESC exhibits brighter EL intensity growing with time and poling cycles due to anion segregation, since EL is governed by I-rich regions that collect radiative excitons by lower band gap [26]. This new photo-poling approach introduces the use of the internal ionic migration doping stages for tuning for better EL, similarly to ionic diffusion in light emitting electrochemical cells [29,30].

2. Experimental details

2.1. Device fabrication

Perovskite based planar p-i-n devices were fabricated in nitrogen atmosphere. For the device fabrication the following scheme of functional layers ITO/PEDOT:PSS/$MAPbBr_2I$/PCBM/LiF/Ag was chosen. The Device functional layers were subsequently deposited onto ITO covered glass substrates. Glass substrates with ITO pixels were cleaned in an ultrasound bath in deionized water, dimethylformamide, toluene, acetone and isopropyl alcohol consequently. Dried substrates were exposed to UV irradiation (189, 254 nm) for 900 s. Water dispersion of PEDOT:PSS 4083 was used as a HTL. It was filtered through PTFE 0.45 syringe filter and deposited by spin coating and annealed on a heating plate for 600 s at 100 °C in ambient atmosphere. A photoactive layer based on $MAPbBr_2I$ was prepared by the consequent dissolving MAI (DyeSol) and $PbBr_2$ (Alfa Aesar "Puratronic" 99,999%) in DMF:DMSO (7:3) respectively. The solutions were steered overnight until dissolved at room temperature. The acquired perovskite inks were deposited by the single step solvent engineering technique [31] on top of HTL in 2 step spin-cycle. Diethyl ether was used as antisolvent and was slowly dripped on the rotating substrate in 10 s past the jumping from 1000 to 2000 rpm. The acquired perovskite films were stepwise annealed on the heating plate in dry atmosphere up to 100 °C with 10 °C step. Fullerene related material PCBM or C_{60} were used as ETL. PCBM was dissolved in clorobenzene (20 mg/ml) and filtered through PTFE 0.45 syringe filter. Filtered solution was deposited onto perovskite layer by the spin coating. Layers of LiF (2 nm) and the Ag cathode were deposited onto PCBM. C_{60} was thermally evaporated in the vacuum chamber. The thicknesses of the ETL, perovskite layer, and HTL were measured by stylus profilometry. The thickness of Ag (C_{60}) cathode was *in-situ* controlled by Inficon deposition controller.

2.2. Device characterization

PV characterization was performed by measurements of photocurrent density-voltage (J-V) characteristics (Keithley 2400) of the solar cells. The devices were illuminated through apertures by a solar simulator HAL-320 Asahi Spectra with an Air Mass 1.5 Global (AM 1.5G) spectrum. LED measurements were performed using a Keithley 2400 source-measure unit, fiber spectrometer (Avantes AvaSpec mini) and Ophir Nova II optical power meter.

3. Results and discussion

The switching from PV to LED regime we first demonstrated by multiple cycling of J-V measurements runs of the PV structure based on a mixed halide $MAPbBr_2I$ perovskite with a band gap of 2 eV, aiming to achieve EL in visible range. These results are presented in Fig. 1 showing that stable and quite bright LED can be turned on after J-V runs in the PV mode under 1 sun illumination.

The very first experiments performed at thin 175-nm perovskite film already demonstrated that after cycling in PV regime the device started

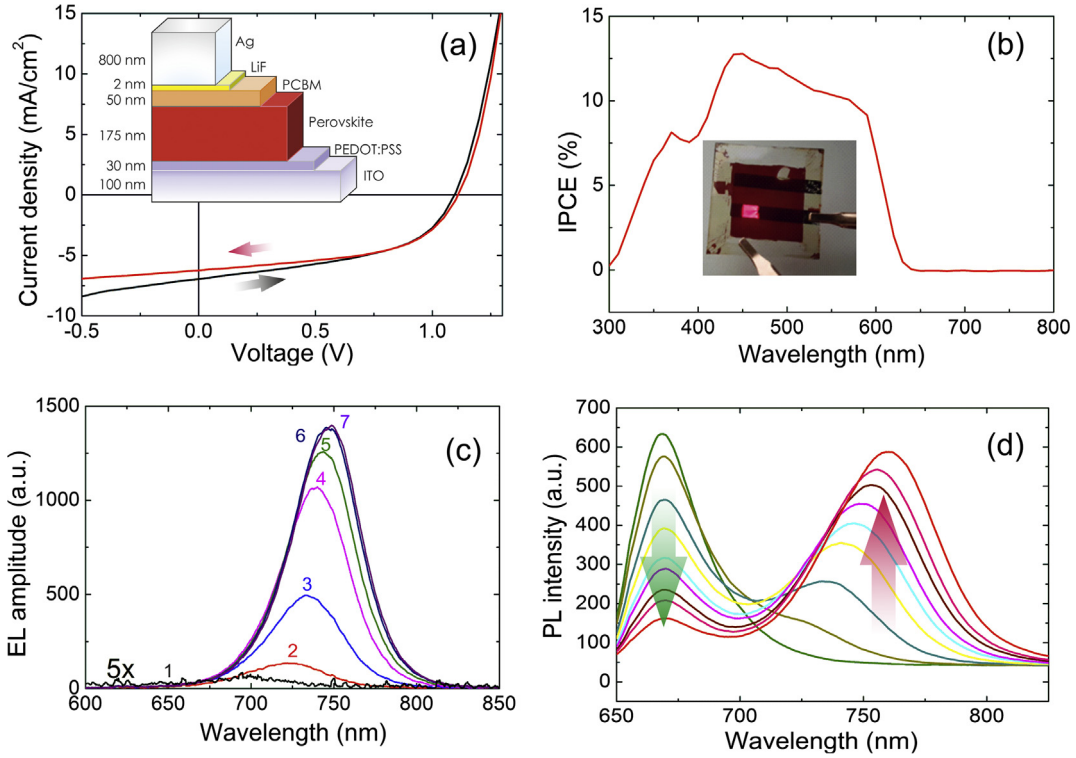

Fig. 1. (a) J-V curves in PV mode and structure of planar LESC device (b) incident photon to current efficiency (IPCE) spectral sensitivity of SC before poling (inset shows a photo of stable LED mode of the device after J-V cycling from −0.5 to +1.5 V). (c) Electroluminescence spectra demonstrate time depended intensity enhancement after switching from SC to LED mode at V_{th} = 2 V. EL curves 1–7 have time step 5 s, black curve has 5× magnification (d) 1-minute photoluminescence time dynamic, showing a strong segregation effect in mixed halide perovskite film.

to give quite bright and stable EL (inset on Fig. 1b). It was evident that exposure to light and some small voltage, can initiate EL in initial PV structure. Without exposure to light the EL regime was either impossible, or if pushed to light up at high threshold voltage (V_{th}) higher than 4 V the device quickly degraded in 1 min (Fig. S1a). On the contrary, after the photo-poling by cycling of J-V runs, the EL was stable and even showed increasing intensity in time. EL spectrum red-shifted from the initial peak at 690 nm and was the brightest at 750 nm (Fig. 1c, S2 and S3), while IPCE of initial SC showed the larger band gap E_g around 2 eV (~600 nm) (Fig. 1b). The photoluminescence (PL) dynamics of mixed halide perovskite film clearly revealed the well-known segregation effect [26]: the shift of the PL peak to the same wavelength range (~750 nm, Fig. 1d and S11) is caused by the domains enriched with I^- ions and thus having lower band gap. Similarity of EL and PL dynamics is clearly observed (Fig. 1c and d). The initial peak at 690 nm disappeared in EL that corresponds to fast and deep segregation enhanced by current injection [25].

3.1. PV performance

First, we studied the evolution of PV parameters upon only photovoltage poling: no external voltage was applied or any J-V cycling done in PV. The real time increase of V_{OC} was observed (inset in Fig. 2a) under continious sun illumination and once J-V characteristic was measured, the improvement was observed not only in V_{OC}, but also in fill factor (FF) and short-circuit current density (J_{SC}) (see Fig. 2a), which resulted in nearly twice improved PCE. This is well known effect of formation of p-i-n junction inside the perovskite layer upon poling first found by Deng [15,28]. Dark J-V curves after V_{OC} poling showed the step like log(J)-V curve, which reflected and confirmed the formation of p-i-n junction, with suppressed current at a small voltage below the internal barrier in p-i-n, and having a step when a voltage above p-i-n barrier (Fig. 2d and c). The increase of V_{OC} upon p-i-n formation can be related to either better interface between n-doped perovskite and ETL by lowering the amount of interfacial traps, or by lowering the barrier at perovskite/ETL interface. Both these arguments imply the possible improved charge injection from the cathode. The photogenerated p-i-n is unstable in darkness and disappears, if PV is shorted [27]. After the relaxation, the new J-V demonstrated its initial low V_{OC} = 0.6 V state and the dark J-V curve goes back to the initial bad diode curve (black curve 1 in Fig. 2b) [15,28].

3.2. LED performance

For the LED operation, we applied forward scan in small electric field and achieved switching to the LED mode by lighting the EL at small turn-on threshold voltage V_{th} (Fig. 2b). The achieved stable EL after photo-poling demonstrated nontrivial time dynamics (Fig. 3b–d). The combined effect of light enhanced ionic migration at higher poling bias of V = 1.5 V and 2 V and photoinduced segregation at prolonged exposure to sun illumination by cycling in PV regime was studied. We observed, that the poling at higher V_{bias} aids to switch EL at lower V_{th}, while V_{th} is also lowered by larger number of cycle runs. We assume that the *in-situ* n-doping of ETL by same ions (MA^+, H^+ and charged vacancies) of perovskite occurs at higher V_{bias} [25,32] and forms the external electronic doping of transport layers: with formation of extended p-(p-i-n)-n junctions. Similarly with I^-, Br^- ions and corresponding charged vacancies, penetrated into the PEDOT:PSS layer by ionic diffusion, induced by external high $V_{bias} > E_g/e$ at sun, is assumed to cause the HTL p-type doping [32]. The electrochemical ionic doping requires charge injection from electrodes (Fig. 4c). On the contrary, photodoping at V_{OC} injects photogenerated charge carriers (Fig. 4b).

Since the LED regime needs higher voltage and higher current densities compared to PV regime, the first task was to keep photodoped p-i-n structure unrelaxed and load it with higher forward V_{bias} in order

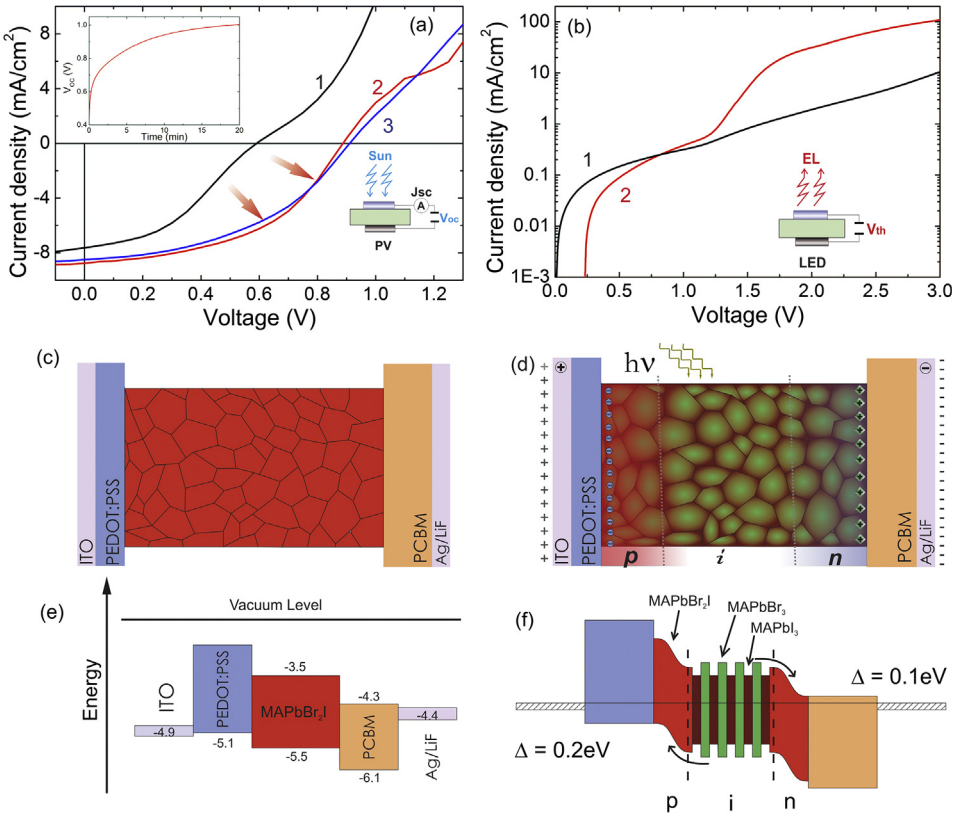

Fig. 2. (a) Self-improvement of V_{OC} under light exposure in the open circuit regime. The upper inset shows the real time measurement of V_{OC} increase under 1 sun. The lower inset with device schematic shows the device working regime. (b) The dark J-V curves of PV before (curve 1) and after self-poling (curve 2). P-i-n junction barrier typically has a "step" shape. Knee in log(J)-V curve corresponds to the straightening of p-n barrier. This allows charge injection in PS layer. The inset with device schematic shows the LED working regime where "+" applied to the ITO and "−" to the Ag electrode (c) The original structure of PV without self-doping (Br^- and I^- ions distributed uniformly). (d) The p-i-n junction is formed by ionic diffusion to interfaces with transport layers. The i-area of p-i-n has segregated regions with I-rich ($E_g \approx 1.57$ eV) and Br-rich ($E_g \approx 2.3$ eV) nanograins, forming an internal bulk heterojunction. EL is enhanced from I-rich regions, by the exciton trapping and energy transfer from green (Br-rich) parts of bulk internal heterojunction. (e) Band diagram of non-segregated device. (f) Band diagram of segregated device: bulk heterojunction marked as alternating green-brown areas.

to turn on the EL mode. Keeping this in mind, the following cycling was studied: after photo-poling at V_{bias}, the external voltage was applied to observe EL. Since the p-i-n structure was stabilized by external V_{bias} the forward scan could be performed until higher V of 4–5 V to observe the EL turning on at certain V_{th}. Indeed, EL was detected at low V_{th} (Fig. 3e) and this cycling of device regimes: photo-poling – LED scan – PV scan can be repeated many times (Figs. S4–S6).

Even a non pre-biased structure can give some unstable EL with very low intensity at high $V_{bias} > 3.5$ V or even higher, which then shows some orange/red light at a very high current of 50 mA (Fig. S2). In this regime, to overcome the high initial barrier for electron injection the very high $V_{th} \sim 4$ V is applied and, in turn, it creates a high unbalanced

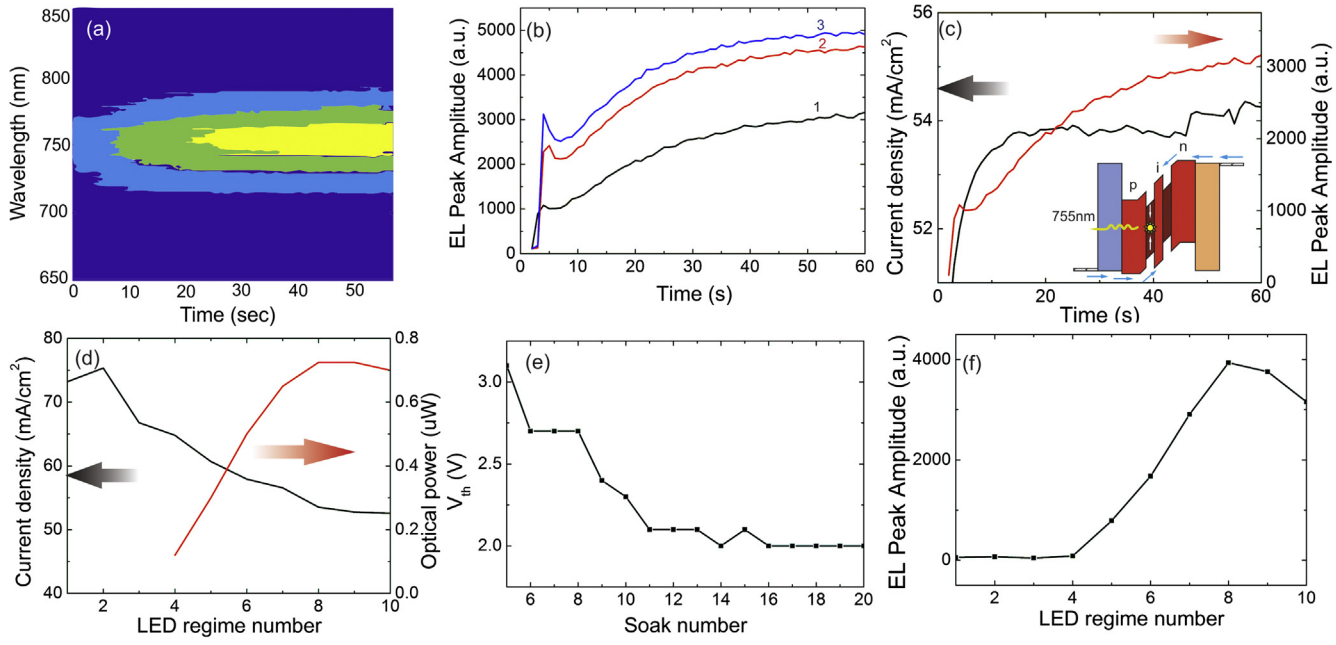

Fig. 3. LED regime turns on by multiple photo-poling cycles: (a) first LED lights up after several soaking cycles at +2 V and 1 sun for 1 min. (b) Enhanced EL amplitude in time measured after 3 soaks at +2 V and 1 Sun. Signs indicate soak number. (c) Time depended current density and EL amplitude plot after soak #2 for LED regime. (d) Current density and LED optical power evolve in the sequence of light soak - LED measurements at +2 V. (e) The decrease of V_{th} value was observed upon 2 V and sun soak cycling. (f) Change in EL peak amplitude depends on number of "light soak – LED" cycles.

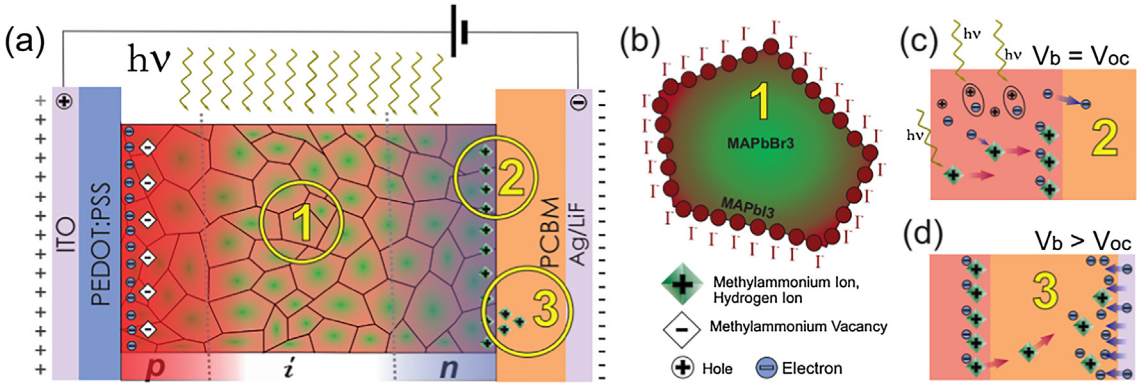

Fig. 4. The device segregation: (a) Schematic illustration of segregation process in the device under 1 sun illumination and applied external voltage. (b) Nanograins of the mixed halide perovskite film undergo segregation upon light and voltage soaking with the development of Br-rich and I-rich regions. (c) Methylammonium and hydrogen accumulation on the interface at V = V_{OC}. (d) Possible Methylammonium penetration into PCBM layer, causing n-doping of ETL at V > V_{OC} via electrochemical charge injection, is assumed to be the origin of improved EL operation at higher bias.

current, which is mostly hole current. Since the device band structure now isn't optimized for charge injection the obtained luminosity and efficiency are very low. The boosted high hole current quickly overheats the device in 1–2 min and it completely degrades. Therefore, fast turned to LED mode PV device, without preliminarily pre-formed p-i-n junction makes the observed low EL absolutely unpractical, since device burns away very fast (Fig. S1a).

On the other hand, the device with the slowly prepared p-i-n structure by photo-poling showed stable EL with self-improving properties (Fig. 3c–d). The spectral shift in EL occurred in time rather fast: the initial EL peak at 690 nm decreased, while intensity of the peak at 750 nm corresponding to I-rich segregated regions increased by about 10 times.

The observed temporal dynamics of EL is quite unusual: EL intensity kept increasing in time during the first minutes of operation at certain V = 2 V. After every cycle of biasing under 1 Sun illumination, the EL peak amplitude increased not only with time but also with cycle number (Fig. 3c). Moreover, the overall optical power also kept increasing from cycle to cycle, the EQE_{EL} efficiency increased up to 0.024% (Fig. S6), which is comparable to EQE_{EL} obtained in low work function Ba-cathode PV device made by Bolink [13].

3.3. p-i-n junction

The increased EL intensity can be explained by two factors: the segregation effect creates the I-rich areas at the interfaces of grains [33], while the Br-rich areas are in the middle parts of grains. The injected carriers are trapped (as radiative excitons) in the low band gap I-rich regions (Fig. 3), and serve as radiative recombination centers for excitons providing effective EL [34,35]. Fig. 3 shows schematics of the segregation influence on EL in the p-i-n junction, which becomes a multiple bulk heterojunction (Fig. 3b).

After switching the device from the PV regime to EL, the observed dynamics of EL is quite complicated, and several effects probably contribute to it. At first stage, the *in-situ* formation of p-i-n in the perovskite layer is critically important. However, applying high V_{bias} and the cycling under high V_{bias} poling had different impacts. As can be seen from the inset on Fig. 4: upon biasing by V_{OC} generated under light soaking the ion migration mainly occurred in perovskite layer, and photogenerated electrons neutralize the accumulated MA^+ ions in the n-type photodoped region of perovskite layer. It should be noted that at this biasing condition, the injection of electrons from Ag cathode to perovskite isn't favorable due to high barrier at the interface of Ag with perovskite. Therefore, the positive charge of MA^+ ions could be compensated only by photogenerated electrons inside perovskite photoactive layer, because the injected electrons cannot support the n-doping within the perovskite layer. Therefore, the V_{OC} biasing isn't effective to create full p-i-n junction and switch to LED mode, and at first stage, only the photogenerated electrons support the internal n-doping in one side of perovskite. Moreover, the light soaking enhances the migration of MA^+ and other ions within the perovskite layer, by the mechanism of lowering the activation barrier [32]. Upon small V_{OC} bias, the photovoltage doesn't create strong enough internal electric E-field inside the ETL, and the ion fast migration within perovskite by photoenhanced diffusion has no driving force to penetrate further into PCBM layer. However, at higher V_{bias} of 2 V, the internal E-field in PCBM most probably pulls MA^+ ions further into the PCBM layer. Also this is a hypothesis at this stage (not yet confirmed by direct measurement of ions present in ETL) for explaining EL improvement dynamics, we believe that this ETL doping is highly preferable by porous structure of fulleride (C_{60} and PCBM) molecular solids. This type of penetration of ions into PCBM [35] and into C_{60} ETLs was demonstrated in [35–40] by external ionic gating in ionic liquids. The MA^+ ions coming from perovskite have smaller size as compared to large ions of ionic liquids, and they can easily penetrate into PCBM, once there is a driving force for this. As it was recently theoretically demonstrated, the optimization of doping level and Fermi level position in transport layers crucially affect the performance of perovskite-based device [18]. Preliminary doping of the transport layers [19] or tuning of Fermi level position inside the transport layers [20] demonstrated good influence for device performance. Therefore, *in-situ* doping of transport layers can indeed aid for better dual functionality. As shown at Fig. 4, the ions are accumulated at the interface of ETL with Ag electrode and create another n-doped layer inside ETL by electrons injected from Ag electrode, since V_{bias} = 2 V is now higher than the electrochemical potential. This second stage doping of ETL (and similarly of HTL on other side) as compared to initial internal doping of perovskite layer itself, further lowers the interfacial barrier, decreases the series resistance, and is most likely to be a reason for the observed decrease of both V_{th} and injection current in LED regime.

Thus, we can assume that the formation of secondary poling-induced doping of ETL and HTL creates (HTL p^+)/(p-i-n)/(n^+ ETL) structure with lower injection barriers. The migrated ions in ETL are trapped at defects, and stay in ETL longer time then in the initial perovskite. We believe this is the most likely reason which rigorous conformation requires direct measurements by X-ray diffraction and other dynamical measurements of increased intensity, optical power, and efficiency of EL after multiple poling cycling runs. Finally, Table 1 represents the comparison of different approaches for development of the dual functional LESC devices. It should be noted, that our preliminary results on the dual function LESC based on $MAPbBr_2I$ with non-optimized architecture, poling and exploitation regimes demonstrated

much worse characteristics [41].

4. Conclusion

The photo-poling of mixed halide perovskite SC has been found to be a simple way to switch to LED regime of planar PV device by initiating ionic migration and *in-situ* doping by internal ions. The internal mobile ions within the perovskite layer are redistributed under light soaking, creating both segregation and interfacial photodoped regions, and form p-i-n junction favorable for LED operation. Such LED is similar to light emitting electrochemical cells, with internal ions causing the photo-doping of perovskite layer upon V_{OC} photovoltage. The secondary doping of transport layers (both ETL and HTL) at higher voltage poling and LED operating voltages, with further evolution into the p^+-(p-i-n)-n^+ structure is tentatively suggested to explain the observed dynamics of further EL improvement with time. Repeated multiple photo-poling cycles reversibly decreases SC performance and at the same time improving the brightness and EQE_{EL} efficiency of LED.

To sum up, the proposed LESC device based on mixed halide perovskite can operate in a dual mode: first as a SC, with built in p-i-n junction upon light soaking, that improves its V_{OC} and PCE; and then at higher forward $V_{pol} > V_{oc}$, it can be switched to the LED mode by poling. The removal of external bias leads to backward redistribution of ions to equilibrium $MAPbBr_2I$ in the bulk of mixed halide perovskite layer. Thus, the device can again operate in any of two different regimes. Since the PV recovers its operation under overnight it is ready to operate again as SC, while further PV cycling upon light soaking helps to form a better LED operation. This study gives insight for development of novel energy saving devices like standalone lightning systems for signage or similar niche applications.

Acknowledgment

The work was supported by the Ministry of Education and Science of the Russian Federation (Projects 16.8939.2017/8.9 for optical measurements and 14.Y26.31.0010 for devices fabrication), Russian Foundation for Basic Researches (Project 18-33-00669 for devices characterization) and partial support from the Welch Foundation (Grant AT 1617). D.S. acknowledge the Increase Competitiveness Program of NUST “MISiS” (contract grant number: K2-2017-007).

Appendix A. Supplementary material

Supplementary data to this article can be found online at https://doi.org/10.1016/j.apsusc.2019.01.031.

References

[1] W.S. Yang, B.-W. Park, E.H. Jung, N.J. Jeon, Y.C. Kim, D.U. Lee, S.S. Shin, J. Seo, E.K. Kim, J.H. Noh, Iodide management in formamidinium-lead-halide–based perovskite layers for efficient solar cells, Science 356 (2017) 1376–1379.
[2] B.R. Sutherland, E.H. Sargen, Perovskite photonic sources, Nat. Photon. 10 (2016) 295–302.
[3] D. Bi, W. Tress, M.I. Dar, P. Gao, J. Luo, C. Renevier, K. Schenk, A. Abate, F. Giordano, J.P.C. Baena, J.D. Decoppet, S.M. Zakeeruddin, M.K. Nazeeruddin, M. Grätzel, A. Hagfeldt, Efficient luminescent solar cells based on tailored mixed-cation perovskites, Sci. Adv. 2 (1) (2016) e1501170.
[4] T. Kirchartz, U. Rau, Decreasing radiative recombination coefficients via an indirect band gap in lead halide perovskites, J. Phys. Chem. Lett. 8 (2017) 1265–1271.
[5] X. Zeng, T. Zhou, C. Leng, Z. Zang, M. Wang, W. Hu, X. Tang, S. Lu, L. Fang, M. Zhou, Performance improvement of perovskite solar cells by employing a CdSe quantum dot/PCBM composite as an electron transport layer, J. Mater. Chem. A 5 (2017) 17499–17505.
[6] M. Saliba, T. Matsui, J.Y. Seo, K. Domanski, J.P. Correa-Baena, M.K. Nazeeruddin, S.M. Zakeeruddin, W. Tress, A. Abate, A. Hagfeldt, M. Grätzel, Cesium-containing triple cation perovskite solar cells: improved stability, reproducibility and high efficiency, Energy Environ. Sci. 9 (2016) 1989–1997.
[7] G. Niu, X. Guo, L. Wang, Review of recent progress in chemical stability of perovskite solar cells, J. Mater. Chem. A 3 (2014) 8970–8980.
[8] N. Arora, M.I. Dar, M. Abdi-Jalebi, F. Giordano, N. Pellet, G. Jacopin, R.H. Friend, S.M. Zakeeruddin, M. Grätzel, Intrinsic and extrinsic stability of formamidinium lead bromide perovskite solar cells yielding high photovoltage, Nano Lett. 16 (2016) 7155–7162.
[9] M. Grätzel, The rise of highly efficient and stable perovskite solar cells, Acc. Chem. Res. 50 (2017) 487–491.
[10] G. Grancini, C. Roldán-Carmona, I. Zimmermann, E. Mosconi, X. Lee, D. Martineau, S. Narbey, F. Oswald, F. De Angelis, M. Graetzel, M.K. Nazeeruddin, One-Year stable perovskite solar cells by 2D/3D interface engineering, Nat. Commun. 8 (2017) 15684.
[11] P. Schulz, Interface design for metal halide perovskite solar cells, ACS Energy Lett. 3 (2018) 1287–1293.
[12] A. Swarnkar, A.R. Marshall, E. Sanehira, B. Chernomordik, D. Moore, J. Christians, T. Chakrabarti, J. Luther, Quantum dot–induced phase stabilization of α-CsPbI3 perovskite for high-efficiency photovoltaics, Science 354 (6308) (2016) 92–95.
[13] L. Gil-Escrig, G. Longo, A. Pertegás, C. Roldán-Carmona, A. Soriano, M. Sessolo, H.J. Bolink, Efficient photovoltaic and electroluminescent perovskite devices, Chem. Commun. 51 (2015) 569–571.
[14] H.B. Kim, Y.J. Yoon, J. Jeong, J. Heo, H. Jang, J.H. Seo, B. Walker, J.Y. Kim, Peroptronic devices: perovskite-based light-emitting solar cells, Energy Environ. Sci. 10 (2017) 1950–1957.
[15] A. Cravino, P. Leriche, O. Alévêque, S. Roquet, J. Roncali, Light-emitting organic solar cells based on a 3D conjugated system with internal charge transfer, Adv. Mater. 18 (2006) 3033–3037.
[16] Y. Deng, Z. Xiao, J. Huang, Light-induced self-poling effect on organometal trihalide perovskite solar cells for increased device efficiency and stability, Adv. Energy Mater. 5 (2015) 1500721.
[17] C. Eames, J.M. Frost, P.R. Barnes, B.C. O'regan, A. Walsh, M.S. Islam, Ionic transport in hybrid lead iodide perovskite solar cells, Nat. Commun. 6 (2015) 7497.
[18] L. Xu, R.M. Imenabadi, W.G. Vandenberghe, J.W. Hsu, Minimizing performance degradation induced by interfacial recombination in perovskite solar cells through tailoring of the transport layer electronic properties, APL Mater. 6 (2018) 036104.
[19] Z. Xu, X. Yin, Y. Guo, Y. Pu, M. He, Ru-Doping in TiO_2 electron transport layers of planar heterojunction perovskite solar cells for enhanced performance, J. Mater. Chem. C 6 (2018) 4746–4752.
[20] Z. Xu, W. Jihuai, W. Tongyue, B. Quanlin, H. Xin, I. Zhang, L. Jianming, H. Miaoliang, H. Yunfang, F. Leqin, Tuning the Fermi level of TiO_2 electron transport layer through europium doping for highly efficient perovskite solar cells, Energy Technol. 5 (2017) 1820–1826.
[21] Z. Xiao, Y. Yuan, Y. Shao, Q. Wang, Q. Dong, C. Bi, P. Sharma, A. Gruverman, J. Huang, Giant switchable photovoltaic effect in organometal trihalide perovskite devices, Nat. Mater. 14 (2014) 193–198.
[22] W. Li, M.U. Rothmann, A. Liu, Z. Wang, Y. Zhang, A.R. Pascoe, Wei Li, Mathias Uller Rothmann, Amelia Liu, Ziyu Wang, J.Lu. Yupeng Zhang, L. Jiang, Y. Chen, F. Huang, Y. Peng, Q. Bao, J. Etheridge, U. Bach, Y.B. Cheng, Phase segregation enhanced ion movement in efficient inorganic CsPbIBr 2 solar cells, Adv. Energy Mater. 7 (2017) 1700946.
[23] W.J. Yin, T. Shi, Y. Yan, Unusual defect physics in CH3NH3PbI3 perovskite solar cell absorber, Appl. Phys. Lett. 104 (2014) 063903.
[24] M. Chen, X. Shan, T. Geske, J. Li, Z. Yu, Manipulating ion migration for highly stable light-emitting diodes with single-crystalline organometal halide perovskite microplatelets, ACS Nano 11 (2017) 6312–6318.
[25] Y.C. Zhao, W.K. Zhou, X. Zhou, K.H. Liu, D.P. Yu, Q. Zhao, Quantification of light-enhanced ionic transport in lead iodide perovskite thin films and its solar cell applications, Light Sci. Appl. 6 (2017) e16243.
[26] E.T. Hoke, D.J. Slotcavage, E.R. Dohner, A.R. Bowring, H.I. Karunadasa, M.D. McGehee, Reversible photo-induced trap formation in mixed-halide hybrid perovskites for photovoltaics, Chem. Sci. 6 (2015) 613–617.
[27] A.J. Barker, A. Sadhanala, F. Deschler, M. Gandini, S.P. Senanayak, P.M. Pearce, E. Mosconi, A. Pearson, Y. Wu, A.R.S. Kandada, T. Leijtens, F. De Angelis, S.E. Dutton, A. Petrozza, R.H. Friend, Defect-assisted photoinduced halide segregation in mixed-halide perovskite thin films, ACS Energy Lett. 2 (2017) 1416–1424.
[28] I.L. Braly, R.J. Stoddard, A. Rajagopal, A.R. Uhl, J.K. Katahara, A.K.-Y. Jen, H.W. Hillhouse, Current-induced phase segregation in mixed halide hybrid perovskites and its impact on two-terminal tandem solar cell design, ACS Energy Lett. 2 (2017) 1841–1847.
[29] S.B. Meier, D. Tordera, A. Pertegas, C. Roldan-Carmona, E. Ort'i, H.J. Bolink, Light-emitting electrochemical cells: recent progress and future prospects, Mater. Today 17 (2014) 217–223.
[30] E. Fresta, Rube'n D. Costa, Beyond traditional light-emitting electrochemical, cells – a review of new device designs and emitters, J. Mater. Chem. C 5 (2017) 5643.
[31] J.-H. Im, H.-S. Kim, N.-G. Park, Morphology-photovoltaic property correlation in perovskite solar cells: one-step versus two-step deposition of CH3NH3PbI3, Appl. Mater. 2 (2014) 081510.
[32] S.J. Yoon, S. Draguta, J.S. Manser, O. Sharia, W.F. Schneider, M. Kuno, P.V. Kamat, Tracking iodide and bromide ion segregation in mixed halide lead perovskites during photoirradiation, ACS Energy Lett. 1 (2016) 290–296.
[33] K. Tvingstedt, O. Malinkiewicz, A. Baumann, C. Deibel, H.J. Snaith, V. Dyakonov, H.J. Bolink, Radiative efficiency of lead iodide based perovskite solar cells, Sci. Rep. 4 (2017) 6071.
[34] C. Zhang, D. Sun, X. Liu, C.X. Sheng, Z.V. Vardeny, Temperature-dependent electric field poling effects in $CH_3NH_3PbI_3$ optoelectronic devices, J. Phys. Chem. Lett. 8 (2017) 1429–1435.
[35] A. Pockett, M.J. Carnie, Ionic influences on recombination in perovskite solar cells, ACS Energy Lett. 2 (2017) 1683–1689.
[36] D. Saranin, A. Ishteev, A.B. Cook, J.D. Yuen, D. Kuznetsov, M. Orlova, S. Didenko, A. Zakhidov, Ionically gated parallel tandem organic solar cells with tunable CNT interlayers, J. Renew. Sustain. Energy 9 (2017) 021204.

[37] D.S. Saranin, P.M. Voroshilov, C.R. Simovski, A.A. Zakhidov, Ionically Gated Small Molecule OPV: Controlled n-doping of thick fullerene acceptor layers, available in arXiv (arXiv:1805.10954), 2018.
[38] A. Cook, J.D. Yuen, A. Zakhidov, Ion-Reconfigurable photovoltaic cells, hybrid tandems and photodetectors with CNT ionic gate, US Patent Application, 61, 2012, 732379.
[39] A.B. Cook, J.D. Yuen, A.A. Zakhidov, Electrochemically gated organic photovoltaic with tunable carbon nanotube cathodes, Appl. Phys. Lett. 103 (2013) 163301.
[40] A.B. Cook, J.D. Yuen, J.W. Micheli, A.G. Nasibulin, A.A. Zakhidov, Ambient method for the production of an ionically gated carbon nanotube common cathode in tandem organic solar cells, J. Visual Experim. 93 (2014) e52380.
[41] D. Gets, A. Ishteev, E. Danilovskiy, D. Saranin, R. Haroldson, S. Makarov, A. Zakhidov, J. Phys. 1124 (2018) 041022.